

An evaluation analysis method for corrosion morphology characterization based on Gaussian filter

ZHANG Peng (张鹏)¹, GUO Bin (郭斌)², CHENG Shu-kang (程树康)³

1. School of Materials Science and Engineering, Harbin Institute of Technology at Weihai, Weihai 264209, China;
2. School of Materials Science and Engineering, Harbin Institute of Technology, Harbin 150001, China;
3. Institute of Electromagnetic and Electronic Technology, Harbin Institute of Technology, Harbin 150001, China

Received 10 June 2009; accepted 15 August 2009

Abstract: The corrosion process of copper in thermal flow system was investigated through the experimental bench. According to surface variation of samples during corrosion process, the surface model of specimen was build up based on Gaussian filter. The results show that the corrosion characterization of copper in thermal flow system is pitting corrosion. The morphology characterizations of metal corrosion process can be described using the proposed surface model. The generation and development of copper pitting process can be observed clearly.

Key words: corrosion; corrosion morphology; Gaussian filter; copper

1 Introduction

Corrosion can range from highly uniform to local extremely during pitting and stress corrosion cracking. In general, corrosion morphologies are rarely uniform. Pits observed on corroded surfaces may be small or large in diameter, which were drawn a variety of sizes and shapes. Therefore, it is of great importance to characterize the corrosion morphology.

Image analysis may be an alternative technique to evaluate corrosion through its morphology characteristics. SINGH and BASW proposed the standard atlas of corrosion morphologies[1]. ITZHAK et al[2] studied pitting corrosion evaluation by computer image processing. MANDELBORT et al[3] studied the metal fracture plane using fractal theory. Then, intercross between fractal theory and conventional method became a new field of corrosion image investigation. CODARO et al[4] analyzed the pitting morphologies characterization through image analysis. WANG et al[5–6] established the corrosion morphology diagnosing system based on the grey value of image element. The corrosion graph data base was studied[7–11]. However, the present image process methods attributes the three

dimensional information through the color and grey value of image element. The original images need quality assurance[12].

In this paper, a method based on Gaussian filter was proposed to attribute the surface variation during the corrosion process. This method was applied in materials with different corrosion degrees.

2 Experimental

2.1 Material and medium

The experimental material was copper. The size of samples was 50 mm × 25 mm × 2 mm. The chemical constitutions of samples were (mass fraction): 99.9% Cu, 0.005% Fe, 0.005% Pb, 0.005% S, 0.06% O, 0.14% Sn, 0.002% As, 0.002% Sb, 0.002% Ni, 0.002% Bi, 0.005% Zn. The weightless samples were sanded to 600#, then defatted, cleaned and dried. The experimental medium was artificial sea water deployed with marine salt.

2.2 Experimental equipment

Fig.1 shows the flow chart of flow corrosion experiment. The magnetic was 0.2 T, the frequency was 150 Hz, the bulk of tank was 200 L, and the flow rate was 0.5 m³/h. The artificial sea water was injected into

the tank, entered into the conduit with the pump and influenced by the electromagnetic field, then loop back to the tank.

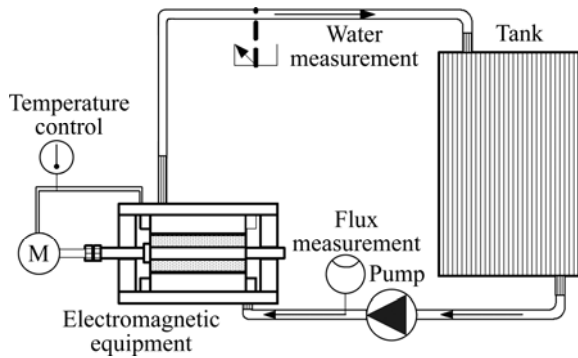


Fig.1 Flow chart of flow corrosion experiment

2.3 Testing method

The three dimensional surface morphology of the samples was observed and estimated by confocal laser scanning microscope (Olympus OLS3000, Japan), which used advanced image processing software and allowed the construction of three dimensional images of the object, topographical maps and quantification of surface topography.

3 Results and discussion

Fig.2 shows three dimensional surface morphologies of copper. It can be observed that there are many pores homogeneously distributed in the surface of samples.

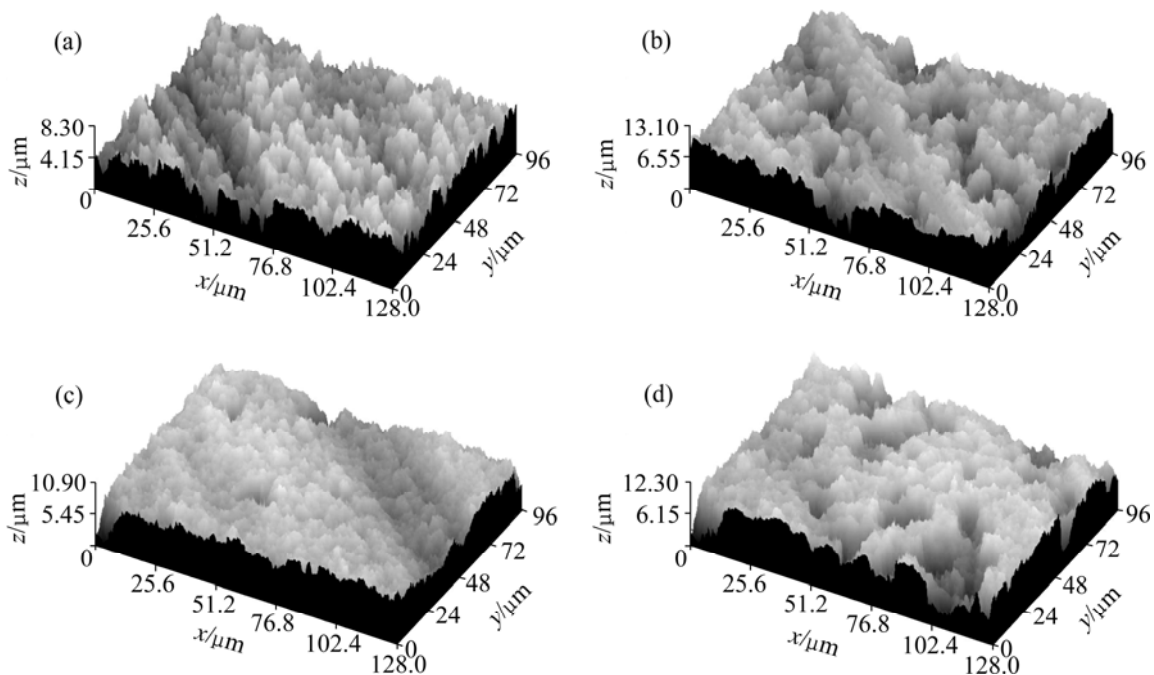


Fig.2 3D morphologies of copper during corrosion process: (a) 3 d; (b) 6 d; (c) 9 d; (d) 12 d

The specimen corroded for three days was pitting corrosion. However, the surface of sample corroded for 9 d formed the protective film owing to continuous deposition of corrosion products. So, corrosion was restrained. Then, specimen surface dissolved and the pit depth increased during the corrosion process.

Fig.3 shows surface roughness of samples corroded for 3 d. It can be observed that the samples surface is highly irregular.

The essence of metal corrosion is electrochemical process. So, the surface irregularity of corroding electrode can influence the mass transport process of the interface between electrode and solution. At the same time, electric double layer can be formed in holes due to the surface irregularity of corroding electrode. Electric double layer in holes will be weakened due to mutual overlap when the size of holes and the thickness of electric double layer are equivalent in magnitude. Overlap effect of electric double layer is to be found in the micropores (< 2 nm) and partial mesopores (2-5 nm). The pores (< 100 nm) occur on the surface of samples during corrosion process. So, the effects of overlap effect on the surface variation of samples during corrosion process should be neglected.

4 Surface model during corrosion process based on Gaussian filter

According to surface variation of samples during corrosion process, the surface model based on Gaussian filter was proposed.

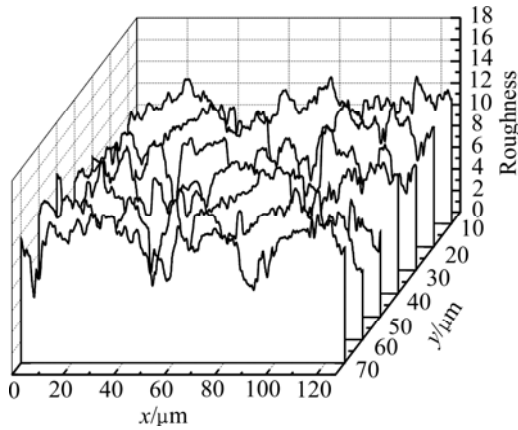


Fig.3 Surface roughness of samples corroded for 3 d

4.1 Theories of Gaussian filter

Gaussian assessment is the configuration obtained through convolution between measured data and Gaussian weight function. In international criterion ISO, Gaussian weight function can be defined as[13–14]

$$g(x) = \frac{1}{a\lambda_c} \exp \left[-\pi \left(\frac{x}{a\lambda_c} \right)^2 \right] \tag{1}$$

Fourier transform can be written as

$$G(\lambda) = \exp \left[-\pi \left(\frac{a\lambda_c}{\lambda} \right)^2 \right] \tag{2}$$

where λ is wavelength; λ_c is close wavelength of filter.

When $\lambda = \lambda_c$, $G(\lambda) = 0.5$, then,

$$a = \sqrt{\frac{\log 2}{\pi}} = 0.469 \ 7 \tag{3}$$

Gaussian fiducial line $w(x)$ can be defined as

$$w(x) = \int_{-\infty}^{\infty} f(\xi)g(x-\xi)d\xi = \int_{-\infty}^{\infty} g(\xi)f(x-\xi)d\xi \tag{4}$$

For three dimensional reference surface, $f(x, y)$ can be defined as three dimensional surface profile.

$$f(x, y) = s_1(x, y) + s_2(x, y) \tag{5}$$

$$S_1(\omega_x, \omega_y) = \begin{cases} F(\omega_x, \omega_y), & |\omega_x| \leq \omega_{cx}; |\omega_y| \leq \omega_{cy} \\ 0, & |\omega_x| > \omega_{cx}; |\omega_y| > \omega_{cy} \end{cases}$$

$$S_2(\omega_x, \omega_y) = \begin{cases} F(\omega_x, \omega_y), & |\omega_x| > \omega_{cx}; |\omega_y| > \omega_{cy} \\ 0, & |\omega_x| \leq \omega_{cx}; |\omega_y| \leq \omega_{cy} \end{cases} \tag{6}$$

where $S_1(\omega_x, \omega_y)$ and $S_2(\omega_x, \omega_y)$ are the Fourier transform of $s_1(x, y)$ and $s_2(x, y)$, respectively. ω_{cx} and ω_{cy} are close

frequency of x and y axis of coordinate, respectively.

If close frequency is appropriate, $s_1(x, y)$ can be considered the reference surface, which includes the shape and the waviness error of measure profile. $s_2(x, y)$ is surface profile, which can be written as

$$s_2(x, y) = f(x, y) - s_1(x, y) \tag{7}$$

Three dimensional measurement profile signals contain various frequency components. The reference surface can be obtained through a two dimensional low frequency filter.

$$\begin{cases} s_1(x, y) = f(x, y) \cdot h(x, y) \\ S_1(\omega_x, \omega_y) = F(\omega_x, \omega_y) \cdot H(\omega_x, \omega_y) \end{cases} \tag{8}$$

$H(\omega_x, \omega_y)$ is Fourier transform of filter impulse response function.

$$H(\omega_x, \omega_y) = \begin{cases} 1, & \sqrt{\omega_x^2 + \omega_y^2} \leq \omega_c \\ 0, & \sqrt{\omega_x^2 + \omega_y^2} > \omega_c \end{cases} \tag{9}$$

$h(x, y)$ of Eq.(8) can be replaced by two dimensional Gaussian function $g(x, y)$. Then,

$$g(x) = \frac{1}{a^2 \lambda_{cx} \lambda_{cy}} \exp \left[-\pi \left(\frac{x}{a\lambda_{cx}} \right)^2 - \pi \left(\frac{y}{a\lambda_{cy}} \right)^2 \right] \tag{10}$$

$$G(x) = \exp \left[-\pi \left(\frac{a\lambda_{cx}}{\lambda_x} \right)^2 - \pi \left(\frac{a\lambda_{cy}}{\lambda_y} \right)^2 \right] \tag{11}$$

Gaussian reference surface $w(x, y)$ can be defined as

$$w(x, y) = f(x, y) \cdot g(x, y) =$$

$$\begin{aligned} & \int_{-\infty}^{\infty} \int_{-\infty}^{\infty} f(\xi, \eta)g(x-\xi, y-\eta)d\xi d\eta = \\ & \int_{-\infty}^{\infty} \int_{-\infty}^{\infty} g(\xi, \eta)f(x-\xi, y-\eta)d\xi d\eta \end{aligned} \tag{12}$$

$$W(\lambda_x, \lambda_y) = F(\lambda_x, \lambda_y)G(\lambda_x, \lambda_y) \tag{13}$$

The proposed surface model can be calculated using the convolution method in Ref.[15].

Fig.4 shows the surface variation of copper during corrosion process. The generation and development process of pitting can be observed.

4.2 Variation of superficial area

The variation of surface area during corrosion process calculated through proposed model are shown in Fig.5. It can be seen that surface area changes due to generation of corrosion. Surface area increases due to generation and development of pitting. Surface area decreases because of surface dissolution of samples.

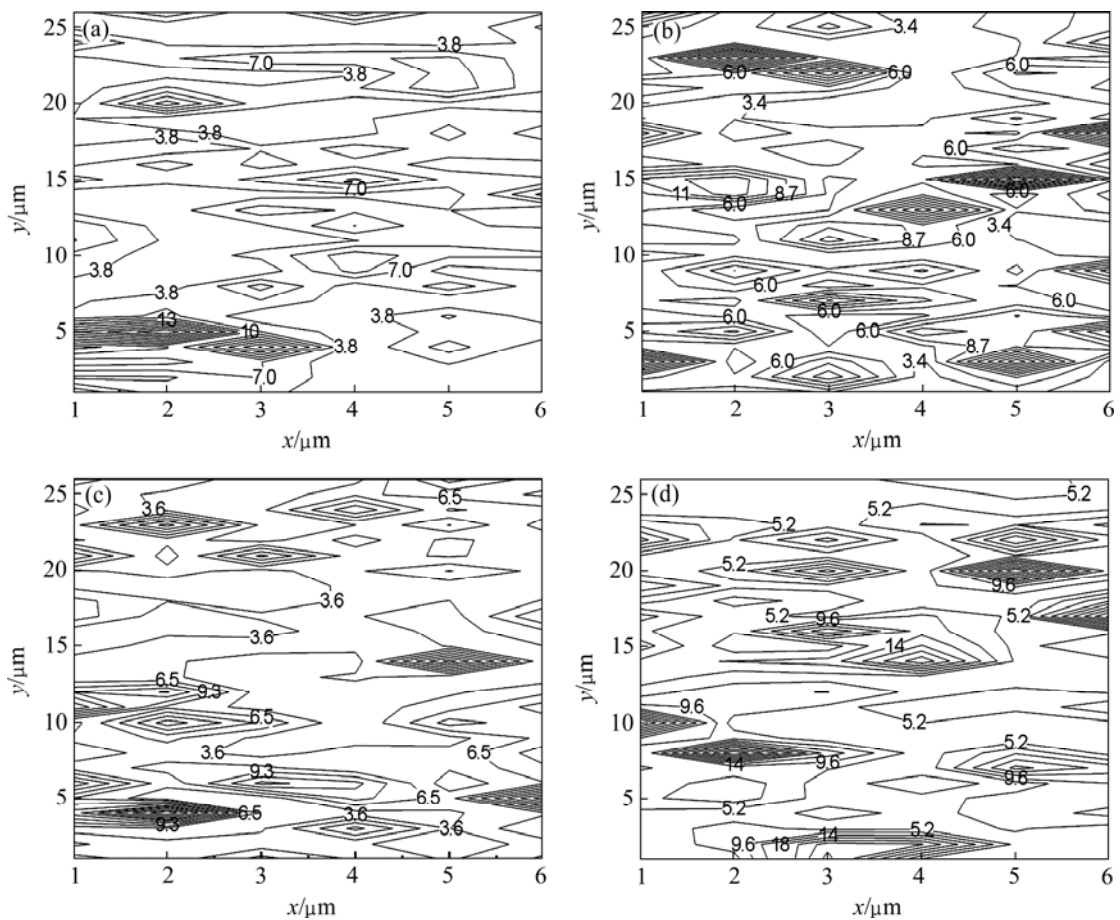


Fig.4 Surface status of samples corrosion process: (a) 3 d; (b) 6 d; (c) 9 d; (d) 12 d

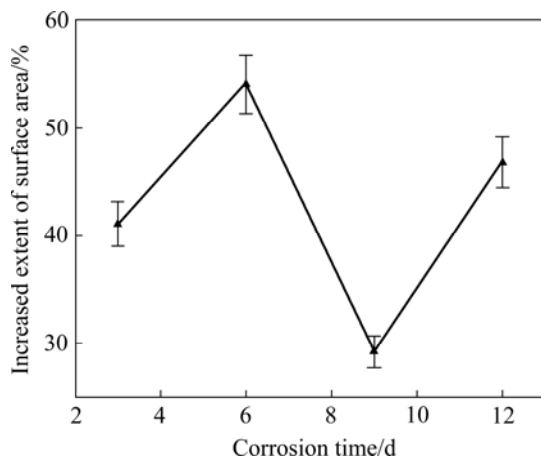


Fig.5 Variation of surface area of samples during the corrosion process

5 Conclusions

1) The flow corrosion process of copper is pitting. The pitting corrosion is restrained owing to continuous deposition of corrosion products. But the copper is dissolved and the pit depth increases during the corrosion process.

2) According to surface variation of samples during

corrosion process, the surface model is build based on Gaussian filter. The proposed model can describe the surface variation of copper during corrosion process.

References

- [1] SINGH S, BASU S. Microscopic characterization of corrosion morphology: A study in specular and diffuse neutron reflectivity[J]. Surface Science, 2006, 600(2): 493–496.
- [2] ITZHAK D, DINSTEIN I, ZILBERBERG T. Pitting corrosion evaluation by computer image processing[J]. Corrosion Science, 1981, 21(1): 17–22.
- [3] MANDELROT B B, PASSOJA D E, PAULLAY A. Fractal character of fracture surface of metals[J]. NACE, 1984, 308(19): 721–722.
- [4] CODARO E N, NAKAZATO R Z, HOROVISTIZ A L. An image processing method for morphology characterization and pitting corrosion evaluation[J]. Materials Science and Engineering A, 2002, 334(1/2): 298–306.
- [5] WANG S Y, SONG S Z. Corrosion morphology diagnosing system of metallic materials in seawater based on fractal[J]. Acta Metallurgical Sinica, 2004, 40(1): 94–98. (in Chinese)
- [6] SONG S Z, WANG S Y, GONG Z M. Atmospheric forepart corrosion behaviors of nonferrous metal based on image recognition[J]. Acta Metallurgical Sinica, 2002, 38(8): 893–896. (in Chinese)
- [7] MIKHAILOV A S, SCULLY J R, HUDSON J L. Nonequilibrium collective phenomena in the onset of pitting corrosion[J]. Surface

- Science, 2009, 603(10/12): 1912–1921.
- [8] CHOI K Y, KIM S S. Morphological analysis and classification of types of surface corrosion damage by digital image processing[J]. Corrosion Science, 2005, 47(1): 1–15.
- [9] CHOI K Y, GRIGORIEV A Y, MYSHKIN N K. Analysis of tribochemical surface damage by image processing[J]. Tribology Letter, 2002, 1(2): 125–129.
- [10] de Carvalho M A G, Lotufo R A, Couprie M. Morphological segmentation of yeast by image analysis[J]. Image and Vision Computing, 2007, 25(1): 34–39.
- [11] GUO Bin, ZHANG Peng, JIN Yong-ping, CHENG Shu-kang. Effect of alternating magnetic field on the corrosion rate and corrosion products compositions of copper[J]. Rare Metals, 2008, 27(3): 324–328
- [12] ZHANG Peng, GUO Bin, JIN Yong-ping, CHENG Shu-kang. Corrosion characteristics of copper in magnetized sea water[J]. Transactions of Nonferrous Metals Society of China, 2007, 17: s189–s193.
- [13] HAN Xu-jun, LI Xin. An evaluation of the nonlinear/non-Gaussian filters for the sequential data assimilation[J]. Remote Sensing of Environment, 2008, 112(4): 1434–1449.
- [14] LAUVERNET C, BRANKART J M, CASTRUCCIO F, BROQUET G, BRASSEUR P, VERRON J. A truncated Gaussian filter for data assimilation with inequality constraints: Application to the hydrostatic stability condition in ocean models[J]. Ocean Modelling, 2009, 27(1/2): 1–17.
- [15] BUDHIRAJA A, CHEN L, LEE C. A survey of numerical methods for nonlinear filtering problems[J]. Physica D, 2007, 230: 27–36.

(Edited by ZHAO Jun)